Articles

Molecular Dynamics Studies of the Kinetics of Phase Changes in Clusters IV: Crystal Nucleation from Molten $(NaCl)_{256}$ and $(NaCl)_{500}$ Clusters

LI, Xiao-Hua[a] **(李小华)** **HUANG, Jin-Fan**[*,b] **(黄锦凡)**

[a] *Department of Chemistry, Nanjing Xiaozhuang College, Nanjing, Jiangsu 210017, China*

[b] *Department of Chemistry, University of Michigan, Ann Arbor, MI 48109, USA*

Molecular dynamics computer simulation based on the Born-Mayer-Huggins potential function has been carried out to study the effects of cluster size and temperature on the nucleation rate of sodium chloride clusters in the temperature range of 580 K to 630 K. Clusters with 256 and 500 NaCl molecules have been studied and the results have been compared with those obtained from 108 molecule clusters. The melting point (*MP*) of the clusters were observed to increase with the size of the clusters and can be well described by a linear equation $MP = 1107(37) - 1229(23)N^{-1/3}$ (*N* is the number of molecules in the cluster). The nucleation rate was found to decrease with increasing the cluster size or temperature. Various nucleation theories have been used to interpret the nucleation rates obtained from this molecular dynamics simulation. It is possible to use a constant diffuse interface thickness to interpret the nucleation rate from the diffuse interface theory in the temperature range of this study. However, the interfacial free energy estimated from classical nucleation theory and diffuse interface theory increases too fast with increasing the temperature while that from Gran-Gunton theory does not change with changing temperatures. The sizes of critical nuclei estimated from all the theories are smaller than those estimated from our simulations.

Keywords sodium chloride, crystal nucleation rate, interfacial free energy, size dependence, temperature dependence

Introduction

Our research work on the nucleation kinetics of phase transitions in condensed matter mainly employed electron diffraction (ED) experiments and/or computational experiments on the basis of the clusters. Clusters studied in ED experiments are generated from supersonic jet expansions with sizes ranging from several nm to around 100 nm.[1-7] Clusters used in computational experiments are usually smaller than 20 nm.[8-10b] The combination of the two approaches benefits us for the better understanding of the current status of the nucleation theories. However, the difference in the cluster size from the two approaches leaves us to study the size effect on the nucleation topic.

The research work on the nucleation and crystallization of alkali halide materials has been a very attractive topic both for science and technology due to alkali halides are widely used as optical materials. Buckle *et al*.[11] started the nucleation of crystallization of alkali halides in high temperature cloud chamber in early 60's. Our series papers on RbCl system[9a,9b] and KI system[10a,10b] provided us a broad view in the nucleation of crystallization in ionic system and the size effect on the nucleation rate in those systems. Molecular dynamics (MD) studies on $(NaCl)_{108}$ reported in our previous papers[12,13] allows us to investigate the nucleation of freezing of $(NaCl)_{108}$ in the temperature range of 400 to 580 K. It is difficult to observe the crystallization above 580 K in a reasonable simulation time period on $(NaCl)_{108}$. To study the size effect and the temperature dependence of the nucleation we performed MD studies on larger clusters and at higher temperatures. In this paper the MD results on $(NaCl)_{256}$ and $(NaCl)_{500}$ clusters in the temperature range of 580 K to 630 K are reported.

Computational procedure

Model and simulation

The MD simulations were performed on the clusters by using a modified version of the program MDIONS[14] in which the leapfrog algorithm was used to propagate the system's evolution. Configurational energies of a rock salt ionic cluster considerably depend on its shape. As it was pointed out in our previous papers the cubic shaped rock salt ionic cluster has the lowest configuration energy and therefore the cubic shape cluster was chosen as the starting point. The initial configuration was based on the face center cubic cell with Na^+ at (0,0,0), Cl^- at (1/2,1/2,1/2), and cell dimension of 0.5641 nm which was determined at 299 K.[15] Equal numbers of Na^+ and Cl^- ions were initially arranged in a cubic shape cluster with each edge length of 4 and 5 times the unit cell resulting in (Na-

* E-mail: jinfanh@umich.edu; Tel.: 1-734-936-2518; Fax: 1-734-647-4865

Received May 29, 2003; revised and accepted September 7, 2003.

Project supported by an NSF founnation of USA to the University of Michigan and Nanjing Xiaozhuang College of China.

$Cl)_{256}$ and $(NaCl)_{500}$ respectively. The interaction potential used was Born-Mayer-Huggins' type[16-19]

$$U = \sum \{q_i q_j r_{ij} - 1 + A_{ij} \exp[(\sigma_{ij} - r_{ij})/\rho]\} \quad (1)$$

where the first term is a simple Coulomb interaction and the second is a repulsive interaction in the short range, which caused from the overlap of the filled electronic shells of the ions. Here q_i and q_j are the charges on the ions i and j, r_{ij} represents the distance between ions i and j. The values of constants A_{ij}, σ_{ij}, and ρ are the same as those used in our previous paper.[12,13]

One of the most important considerations in nucleation studies of phase transition from molten state to solid state is to generate the liquid without any critical nucleus of solid phase. Such kind of liquid can be obtained by heating the cluster well above its melting point for certain amount of the time. Melting point of small clusters depends on their sizes. Therefore studying the melting point is the first step in our MD simulation on nucleation. A normal process in our simulation is to heat the cluster up by keeping it in a heat bath for certain amount of time steps followed by constant energy simulation. A temperature fluctuation limit of 4 K was set when the cluster was kept in the heat bath. Temperature scaling was performed once the temperature difference between the system and the bath exceeds the limit. The simulation for both clusters was started with 5000 time steps in a bath of 298.15 K and followed by another 5000 time steps at constant energy, then repeated 5000 time steps in a bath at 298.15 K and 10000 time steps at constant energy. A series of heating stages then began at 320 K, and each succeeding stage is 20 degree warmer than the previous one. Every stage was first simulated at constant temperature for 5000 time steps and then by 5000 time steps at constant energy. Heating was continued to 1100 K, which is *ca*. 30 K above the melting point of the bulk.

Freezing was simulated in the similar way used in the melting process. Melted clusters were cooled through a series of stages started from 1020 K and 1090 K for $(NaCl)_{256}$ and $(NaCl)_{500}$ respectively, each succeeding stage is 20 degree cooler than the previous one until the clusters reached 320 K. Such a process corresponds to a heating/cooling rate of 2.5×10^{11} K/s.

A similar heating and cooling process was performed on $(NaCl)_{108}$ cluster to compare with our previous results of $(NaCl)_{108}$ cluster, where a heating/cooling rate of 5.0×10^{11} K/s was used and longer heating time around the melting point was tested.

Because of the stochastic character of crystal nucleation, the detailed nucleation rate analysis of crystallization from the liquid should be evaluated from a certain number of nucleation events starting from completely melted systems with different thermal histories. Such kind of systems were first generated from the heating process mentioned above. After the $(NaCl)_{256}$ cluster was melted from the melting process at 1000 K as mentioned above it was directly heated in a bath of 1010 K for 5000 time steps and followed by another 5000 time steps at the constant energy simulation, then the cluster was heated in the heat bath of 1010 K for another 32000 time steps. The heating was continued at 1030 K to form 16 clusters each with 2000 more time steps than the previous one that gave 16 melted systems with different thermal histories for crystal nucleation studies. The heating process for $(NaCl)_{500}$ cluster was followed from that of 1060 K described above and then kept in a bath of 1070 K for 5000 time steps and followed by another 5000 time steps at the constant energy simulation, then the cluster was heated in the heat bath of 1070 K for 32000 more time steps. Sixteen melted systems of $(NaCl)_{500}$ cluster with different thermal histories were generated in the similar way but at a much higher temperature (1090 K). There is no critical nuclei left for all the molten systems generated in this way. It is based on the diagnosis that will be described later. In all the simulations time step size was set at 8 fs.

Nucleation rates were investigated by immediately quenching the melted clusters into a heat bath at the temperature of interest. The first temperature was chosen at 580 K which is the highest temperature, in which $(NaCl)_{108}$ cluster could be crystallized at a reasonable length of simulation time in our previous work.[12,13] On other hand, $(NaCl)_{256}$ and $(NaCl)_{500}$ clusters readily freeze into polycrystalline solid below this temperature. The highest temperature was chosen at 630 K, above this limit it is difficult to observe crystallization within a reasonable length of simulation time even for $(NaCl)_{500}$ cluster. Another temperature, 615 K, was chosen between the two limits. Two melted $(NaCl)_{108}$ clusters were not crystallized at 580 K within the time limit of 240 ps in our previous reports. For the purpose of comparing the size effect on the nucleation rate, we continued the cooling process of these uncrystallized systems of $(NaCl)_{108}$ at 580 K until the crystallization was observed.

Diagnosis of melting and freezing

In our previous simulation on $(NaCl)_{108}$ cluster various diagnostic tests were applied during the heating and cooling process to monitor the behavior of ions. Melting and freezing were ascertained by observing the temperature dependence of caloric curve, the Lindemann index δ^*, and the pair correlation function $g(r)$. All these three criteria gave the similar melting point of $(NaCl)_{108}$ cluster, therefore only caloric curves were used to determine the melting point for different size of clusters. MACSPIN program[9b] offers a very convenient way to view the image of the arrangement of ions and to monitor the progress of a phase change. This is especially useful to identify the nuclei, to monitor the crystal growth process, and to judge whether the final solid cluster is a single crystal or a polycrystalline phase.

The analysis for the nucleation of phase transitions in bulk material to give structural characteristics of very small

region where the potential nuclei for phase transition may present[20,21] was mainly based on Voronoi polyhedral technique in the past years. In our previous paper we proposed a simple method that uses the coordination number of 12 and a cutoff distance which corresponds to the first minimum of the pair-correlation function of equivalent lattice points (in NaCl case are Na^+-Na^+ pairs or Cl^--Cl^- pairs).[12,13] Such a simple method considers polyhedra formed from a central ion and 12 ions of the same type with distances to the central ion shorter than the cutoff distance as the character of the solid phase. It corresponds to taking all distorted Voronoi polyhedra into account and works very well by using the moment of sharp increase in the number of such polyhedra as the starting time of crystal growth in our $(NaCl)_{108}$ study.[12,13] Recently, it was found that this simple method combined with Voronoi polyhedra analysis was useful in determining the nucleation time for different sizes of SeF_6 clusters even though the solid phase crystallized out is "bcc" or monoclinic in this case.[22] We use this simple method in our present work without further modification and refer such polyhedra as "fcc unit".

Estimation of nucleation rate

On the basis of the assumption that the fraction of unfrozen clusters obeys the first order rate law

$$N_n(t_n)/N_0 = \exp[-JV_e(t_n - t_0)] \tag{2}$$

where N_0 is the total number of clusters, J the nucleation rate, V_e the effective volume in nucleation, t_n the time at which the nth nucleation event in the set of N_0 clusters has taken place, t_0 the time lag to achieve a steady state of precritical nuclei, and $N_n(t_n)$ is defined as[22]

$$N_n(t_n) = N_0 - n + \Delta \tag{3}$$

the quantity Δ is taken as 1. Eq. (2) can be written as

$$\ln[N_n(t_n)/N_0] = -JV_e(t_n - t_0)] \tag{4}$$

Therefore from the slope of the curve $\ln[N_n(t_n)/N_0] \sim t_n$ it is able to obtain J, the nucleation rate of freezing. The information about time t_n will be estimated from the sharp increasing in the numbers of "fcc unit" described in the previous section. Because of the uncertainty upon the time of the nucleation events a weighted least square fitting on t_n was carried out to get the nucleation rate. Details of this procedure was given in Ref. 22.

As it will be discussed later to take the total volume of the cluster as the effective volume V_e might be the best way for sodium chloride system based on our current results.

Estimation of interfacial free energy

For a homogenous nucleation the rate can be expressed by[23,24]

$$J(T) = A\exp(-\Delta G^*/k_B T) \tag{5}$$

where k_B is the Boltzman constant, T the temperature, and ΔG^* the free energy barrier to the formation of a critical nucleus from the liquid.

For the classical nucleation theory (CNT) ΔG^* for a spherical nucleus is given by

$$\Delta G^* = 16\pi\sigma_{sl}^3/[3(\Delta G_v + w')^2] \tag{6}$$

where σ_{sl} is the interfacial free energy between solid and liquid, ΔG_v represents the free energy of freezing per unit volume, and w' the work per unit volume of changing the surface area of liquid phase during the formation of the nucleus which is expressed as

$$w' = P_L(\rho_l - \rho_s)/\rho_l \tag{7}$$

where P_L is the Laplace pressure $2\sigma_l/r_0$ inside the cluster and ρ_l and ρ_s are densities of liquid and solid, respectively.

In the Diffuse -Interface theory (here after DIT)[25-28] ΔG^* is given by

$$\Delta G^* = -4\pi\delta^3\Delta G_v\Psi/3 \tag{8}$$

where δ is the thickness of the diffuse interface thickness, and Ψ is defined as[22]

$$\Psi = [2(1+Q)H^{-2} - (3+2Q)H^{-1} + 1]/\eta \tag{9}$$

with $\eta = \Delta G_{fus}/\Delta H_{fus}$, $H = \eta(1+\zeta)$ with $\zeta = w'/\Delta G_v$, and $Q = (1-H)^{1/2}$

Both CNT's and Grant-Gunton's (GG)[29] prefactors were tested. The conventional formula for CNT's prefactor used is

$$A_{cl} = 16(3/4\pi)^{1/3}(\sigma_{sl}/k_B T)^{1/2} D/v_m^{2/3}\Delta r^2 \tag{10}$$

where D is the coefficient of diffusion in the liquid, v_m is the volume of a molecule in solid, and Δr is the molecular jumper distance from the liquid to solid taken to be $v_m^{1/3}$.

A modified CNT prefactor in DIT theory was used and it will be known as DIT prefactor from now on. Its expression is[30]

$$A_{DIT} = \rho_l O\Gamma Z \tag{11}$$

with $\rho_l = 1/v_m$, $O = 4[4\pi R_s^{*3}/(3v_m)]^{2/3}$, $\Gamma = 6D\lambda^{-2}$, and $Z = [v_m/(2\pi R_s^{*2})][-\Delta G_0(R_s^* - \delta/H)/(k_B T)]^{1/2}$, here R_s^* is the radius of the nuclei which is calculated from $R_s^* = \delta(1+Q)H^{-1}$, λ is the jump distance in the liquid phase, ΔG_0 is the molar free energy difference between the

supercooled liquid and the solid.

The GG prefactor can be expressed as[6]

$$A_{GG} = 1.54\lambda (\sigma_{sl})^{7/2} / [(k_B)^{3/2} T^{1/2} L^2 (-\Delta G_v) \zeta^4] \quad (12)$$

where λ_1, L, and ζ represent the thermal conductivity, heat of fusion per unit volume of solid, and a correlation length characterizing the thickness of the interface between the solid and liquid, respectively. The temperature dependence of ζ was estimated from the resported sesults.[31-33]

Interfacial free energy between the solid and the liquid, σ_{sl}, can be derived from the nucleation rate obtained from our simulation via the combinations of various prefactors with the exponential part from either CNT or DIT.

Results

Melting

The selected images generated from the MACSPIN program for heating and cooling processes of $(NaCl)_{256}$ and $(NaCl)_{500}$ clusters are shown in Fig. 1.

Fig. 2 presents the potential energies of various clusters as a function of temperature. It is obvious that there is no unique temperature corresponding to the transition due to the extremely high heating rate and the large temperature increment between two successive heating runs. We select the midpoint of a jump in the potential energy that occurs when the cluster is being heated. The uncertainty is estimated from the two temperatures around the midpoint of the jump. According to this definition the melting temperatures and associated uncertainties are 851(13), 914(4), and 957(19) K for $(NaCl)_{108}$, $(NaCl)_{256}$, and $(NaCl)_{500}$ respectively under the heating rate mentioned in the previous section.

In Fig. 3 we plot the melting point of the cluster as a function of $N^{-1/3}$ and extended to N equal to infinitive corresponding to the bulk, where N is the number of NaCl molecules in a cluster. It is well within the uncertainty limits, a linear curve fitting of simulated results along with the bulk melting point gives

$$T = 1107(37) - 1229(23) N^{-1/3} \quad (R = 0.996) \quad (13)$$

A common characteristic for the molten NaCl clusters is that they are non-spherical especially for the smaller clusters. The reasons have been given in a recent publication.[34]

Temperatures to generate molten liquid clusters

As it was mentioned above to choose the temperature where the molten liquid systems were generated for nucleation study, the melted system without any critical nuclei was selected. To ensure this criterion was satisfied it is

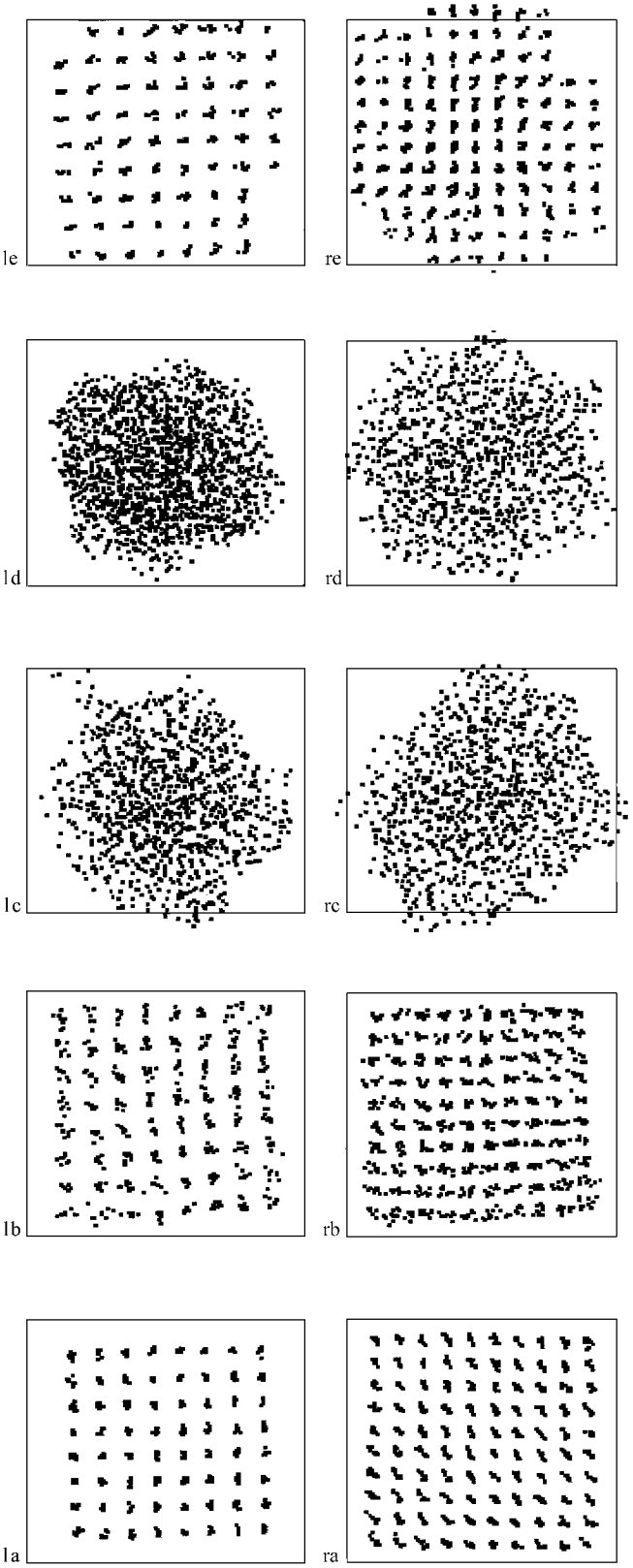

Fig. 1 Images of clusters at various stages of heating (left-hand column) and cooling (right-hand column). Left-hand figures are for $(NaCl)_{256}$ at 320 K (1a), 840 K (1b), 1040 K (1c), 1060 K (1d) and 320 K (cooling) (1e); Right-hand figures are for $(NaCl)_{500}$ at 320 K (ra), 940 K (rb), 1060 K (rc), 1100 K (rd) and 320 K (cooling) (re).

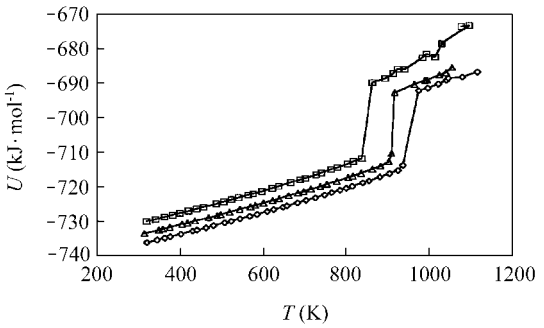

Fig. 2 Potential energy per mole of cluster as a function of temperature during the heating stages. Obtained when the clusters were heated with 10000 time steps at each temperature with 5000 steps in the bath and 5000 steps at constant energy, square for $(NaCl)_{108}$, triangle for $(NaCl)_{256}$, circle for $(NaCl)_{500}$.

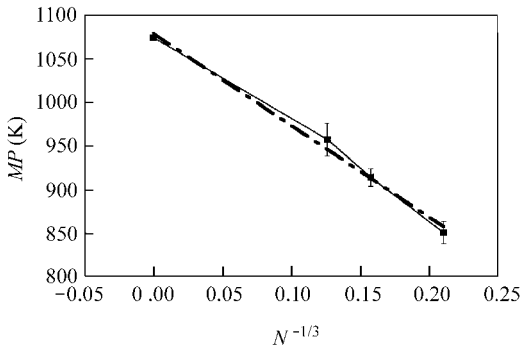

Fig. 3 Size dependence of the melting temperature of NaCl clusters. N is the number of molecules in a cluster.

safer to heat the cluster to the highest temperature we can reach but without vaporizing any molecules. For the $(NaCl)_{256}$ cluster, the highest temperature could be reached is 1030 K without vaporizing any molecules. A temperature of 1000 K was chosen for $(NaCl)_{108}$ cluster with a similar analysis procedure as mentioned.[12] The molten system of $(NaCl)_{500}$ cluster was generated at 1090 K which is *ca*. 15 K above the melting point of the bulk. Diagnoses indicate there is no critical nucleus left in these melted systems.

Freezing

The caloric curves for cooling process of different clusters are given in Fig. 4. The same definition for the melting point to estimate the freezing temperature was described. The estimated values and the deviations are 575(13), 646(21), and 611(22) K for $(NaCl)_{108}$, $(NaCl)_{256}$, and $(NaCl)_{500}$ respectively under the cooling rate of 2.5×10^{11} K/s. Because the stochastic nature of the nucleation initiating a phase change makes the freezing temperature unpredictable and unreproduciable, these temperatures were used only as a reference to set the temperature range for nucleation studies. It was found that if the molten clusters were quenched into a bath with temperatures around the freezing temperature, the liquid crystallizes into single crystals within a reasonable simulation time. If the bath temperature is much lower than the freezing temperature polycrystalline crystals are the main products, however, it is difficult to crystallize the liquid within a reasonable simulation time if the bath temperture is much higher than the freezing temperature.

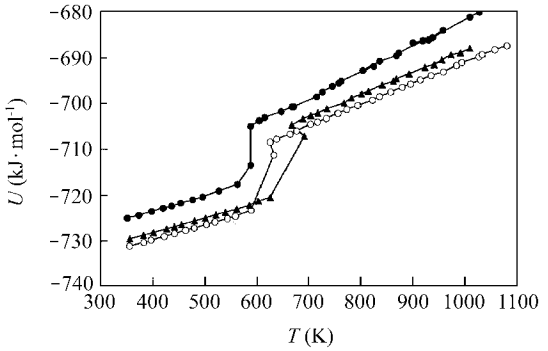

Fig. 4 Potential energy per mole of cluster as a function of temperature during the cooling stages. Filled circle for $(NaCl)_{108}$, filled triangle for $(NaCl)_{256}$, circle for $(NaCl)_{500}$.

As shown in Fig. 1, both $(NaCl)_{256}$ and $(NaCl)_{500}$ clusters freeze into single crystals when they are cooled at the rate of 2.5×10^{11} K/s.

Crystallization of clusters was also observed when all the completely melted clusters are quenched into the bath temperature selected. When the $(NaCl)_{500}$ clusters are quenched into the bath at 630 and 615 K all 32 clusters are frozen into single crystalline phases. However, only 7 of them form single crystals while the remain 9 form polycrystalline phases when they are quenched into the bath at 580 K. All 16 molten $(NaCl)_{256}$ clusters grow into single crystals in the heat bath of 615 K, 15 of them grow into single crystals at 580 K, only one forms a polycrystal. As it was mentioned before[12,13] among the 16 molten $(NaCl)_{108}$ clusters 14 of them formed single crystals at 580 K within the time limit of 240 ps. Two unfrozen $(NaCl)_{108}$ clusters could be crystallized into single crystals in this study by keeping them in the heat bath of 580 K for a longer time.

Nucleation of crystallization

Fig. 5 shows the typical examples of time evolution of the number of "fcc unit" for clusters during the quenching in the heat bath of 580, 615 and 630 K. The t_n value was identified as the time step at which the instantaneous number of "fcc unit" began a concerted ascent. Fig. 6 plots the $\ln[N_n(t_n)/N_0]$ vs. t_n obtained from 96 runs at three different temperatures.

Based on the assumption that take the total volume or the volume of surface molecules of a cluster as the effective volume V_e, the calculated nucleation rates are listed in Table 1. Uncertainties are standard deviations based solely on the counting statistics of Eq. (14) in Ref. 22.

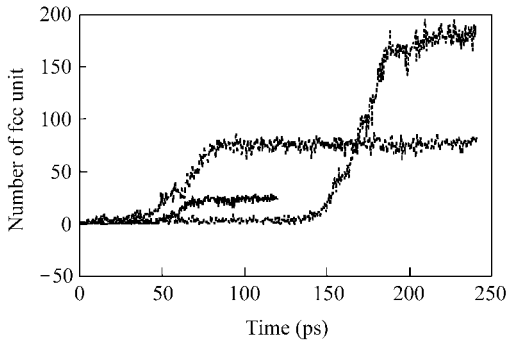

Fig. 5 Evolution of "fcc unit" as a function of time. The curve with maximum at ~25 is from $(NaCl)_{108}$, with maximum at ~75 is from $(NaCl)_{256}$, and with maximum at ~180 is from $(NaCl)_{500}$.

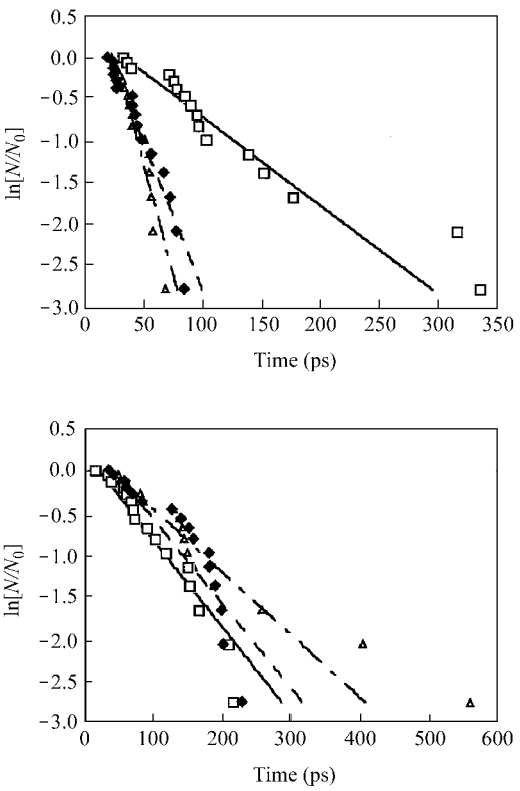

Fig. 6 $\ln[N_n(t)/N_0] \sim t$ plot from 96 MD runs. Top figure is from 580 K, square for $(NaCl)_{108}$, filled square for $(NaCl)_{256}$, triangle for $(NaCl)_{500}$; Bottom figure is from 615 and 630 K, filled square for $(NaCl)_{256}$ at 615, square for $(NaCl)_{500}$ at 615 K, triangle for $(NaCl)_{500}$ at 630 K.

Table 1 Calculated nucleation rate $(m^{-3}\cdot s^{-1})$

Cluster	Temperature		
	580 K	615 K	630 K
From total volume			
$(NaCl)_{108}$	$2.2(0.7)\times10^{36}$		
$(NaCl)_{256}$	$3.4(1.1)\times10^{36}$	$8.9(2.8)\times10^{35}$	
$(NaCl)_{500}$	$2.7(1.8)\times10^{36}$	$4.6(1.4)\times10^{35}$	$3.4(1.1)\times10^{35}$
From the volume of surface molecules			
$(NaCl)_{108}$	$3.1(1.0)\times10^{36}$		
$(NaCl)_{256}$	$5.9(1.9)\times10^{36}$	$1.5(0.5)\times10^{36}$	
$(NaCl)_{500}$	$5.5(1.7)\times10^{36}$	$9.4(2.9)\times10^{35}$	$6.9(2.2)\times10^{35}$

Discussion

Size dependence of nucleation rate

Based on the Eq. (4) that was used for analyzing the nucleation rate from MD simulation, the effective volume, V_e, is the key factor. If the nucleation is initiated everywhere in the whole clusters, the total volume of the cluster should be used as V_e. If it is always initiated in the interior of the cluster, the volume considered to participate in the nucleation will be the difference between the volume of the total volume of the cluster and the volume of the surface molecules. Conversely, if it is always initiated near the surface of the cluster, the V_e will be the volume of several layers of surface molecules. Fig. 7 gives some MACSPIN images of the $(NaCl)_{500}$ clusters that were obtained around the end of nucleation time when they were cooled in the bath of 630 K. It is obvious from these pictures that all the critical nuclei are located near the surface of the clusters. There might be some smaller embryos in the interior of the clusters coexisting with the critical nuclei, however, they disappeared while the critical nucleus grew into crystals. Among the systems given in Fig. 7, new smaller embryos may form and disappear again, but any of them did not become new critical nuclei if the final solid phase is a single crystal. The right column of Fig. 7 may demonstrate a snapshot of this dynamic process. Therefore it seems the best to use the volume of several layers of molecules starting from the surface of the cluster as the effective volume to estimate the nucleation rate from Eq. (4). For small clusters studied in this report this effective volume is very close to the total volume. The nucleation rate were calculated as shown in Table 1, based on the total volume and on an extreme case that only the volume of one layer surface molecules is considered. It is clear that no matter whether the total volume or only the surface volume is taken into account in the calculation, two out of three available data sets give the trend that at the same temperature the nucleation rate slightly decreases with increasing the cluster sizes.

From the viewpoint of nucleation theory expressed in Eqs. (5) to (12) the dependence of nucleation rate on cluster size was mainly caused by the size dependence of property parameters going into these equations. In the exponential part of CNT and DIT the free energy of freezing per unit volume, $\Delta G_v(T)$ in Eqs. (6) and (8) can be estimated from the standard thermodynamics

$$\Delta G_v(T) = (1/V)\int_{Tm}^{T} \Delta S_{fus}(T)\,dT \qquad (14)$$

where V is the molar volume, $\Delta S_{fus}(T)$ the molar entropy change of fusion at temperature T and it can be calculated by the difference between the heat capacities of liquid and solid. The estimated difference of heat capacities from the heating and cooling curve presented in Figs. 2 and 4 for different size clusters is essentially the same.

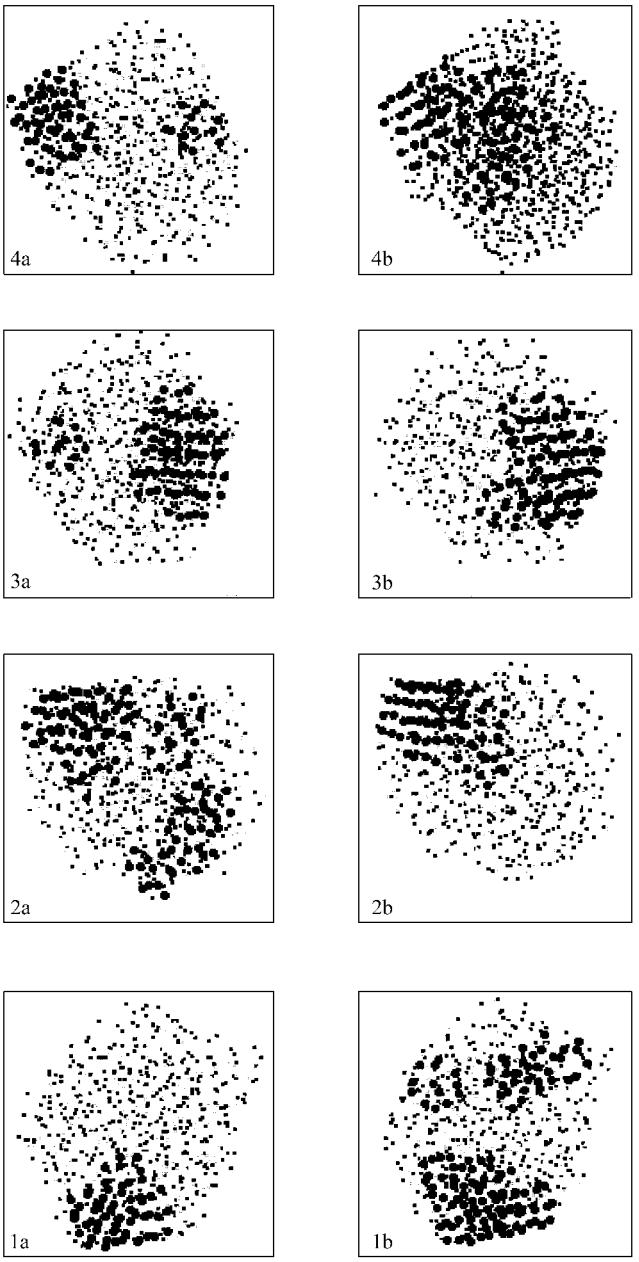

Fig. 7 Evolution of critical nuclei from $(NaCl)_{500}$ at 630 K. Heavy dark spots represent the chlorine ions that satisfy the "fcc unit" (for the definition of "fcc unit" see the text). (1a), Run #1 at 141.6 ps; (1b), Run #1 at 141.6 ps; (2a), Run #2 at 129.2 ps; (2b), Run #2 at 130.8 ps; (3a), Run #3 at 130.0 ps; (3b), Run #3 at 137.2 ps; (4a), Run #4 at 38.4 ps; (4b), Run #4 at 42.40 ps.

Therefore the main size effect in the exponential part of CNT may come from the Laplace pressure contribution, w', given in Eq. (7). The calculation of other terms in ΔG^* for DIT also contains the correction of Laplace pressure that may result in an additional size effect from the exponential part.

Among the parameters going into the CNT prefactor given in Eq. (10), v_m, the volume of a molecule in liquid, will be affected by the Laplace pressure. The diffusion coefficient, D, is also size dependent because smaller clusters usually have larger diffusion coefficient due to the higher percentage of surface molecules. As it is shown in Eq. (11), besides v_m and D, there is H in DIT prefactor which depends on the Laplace pressure. Bigger size dependent effect should be seen from the DIT.

An example of the calculated nucleation rates with and without w' corrections for three different size clusters are listed in Table 2, where the size effect on v_m and D are neglected. Uncertainties in nucleation theory prevents an accurate calculation of the nucleation rate, however, the trends predicted by the theory may make some sense. It seems that both MD simulation and current nucleation theories after Laplace pressure correction follow the same trend that the nucleation rate decreases with increasing the number of molecules in a cluster.

Table 2 Calculated size effect on nucleation rate[a] ($m^{-3}\cdot s^{-1}$) due to the Laplace pressure

Cluster	CNT		DIT	
	with w'	without w'	with w'	without w'
$(NaCl)_{108}$	1.5×10^{37}	7.2×10^{36}	5.3×10^{36}	7.9×10^{35}
$(NaCl)_{256}$	1.3×10^{37}	7.2×10^{36}	3.4×10^{36}	7.9×10^{35}
$(NaCl)_{500}$	1.2×10^{37}	7.2×10^{36}	2.5×10^{36}	7.9×10^{35}

[a] The calculation was based on the following data, temperature T = 580 K, interface thickness in DIT $\delta = 1.493\times10^{-10}$ m, interfacial free energy = 71 mJ/m^2.

Laplace pressure correction for CNT resulted in a factor of *ca*. 2 increase in the nucleation rate. This correction for DIT is even larger, a factor of *ca*. 7 is introduced for $(NaCl)_{108}$ cluster at 580 K.

Interfacial free energy and the diffuse interface thickness

Based on the estimated nucleation rates from MD simulation and thermal properties of sodium chloride listed in Table 3, the free energies between the interface of solid and liquid and the thickness of the diffuse interface are derived from Eqs. (5) to (12) as shown in Table 4.

Table 3 Physical properties of NaCl used in the calculation

Property	Value or expression	Ref.
T_m (K)	1073	CRC handbook
T_b (K)	1738	CRC handbook
ΔH_{fus} (J/mol)	30180	CRC handbook
$C_p(l) - C_p(s)$ (J/mol·K)	17.5	12, 13
V_{ms} (solid) (m^3/mol)	2.67×10^{-5}	CRC handbook
V_{ml} (liquid) (m^3/mol)	3.14×10^{-5}	CRC handbook
λ ($W\cdot m^{-1}\cdot K^{-1}$)	$0.1+0.0008T$ (K)	41,42
D (m^2/s)	$3.1662\times10^{-7}\times\exp(-4089/T)$	43
ζ (nm)	$2.2\times10^{-9}\times(T/T_m)^{1.3}$	31—33
σ_{vl} (J/m^2)	$0.1906-7.125\times10^{-5}T$	44

Table 4 Interfacial free energy and diffuse interface thickness[a]

T/Cluster	CNT		DIT
	$\sigma_{sl}(A_{CNT})$	$\sigma_{sl}(A_{GG})$	δ
580 K			
$(NaCl)_{108}$	0.0830	0.1195	0.1590
$(NaCl)_{256}$	0.0795	0.1165	0.1494
$(NaCl)_{500}$	0.0800	0.1160	0.1488
615 K			
$(NaCl)_{256}$	0.0870	0.1175	0.1512
$(NaCl)_{500}$	0.0885	0.1175	0.1532
630 K			
$(NaCl)_{500}$	0.0895	0.1170	0.1504

[a] The unit for σ_{sl} is in J/m^2, and δ is in nm.

On the basis of the interfacial free energy listed in Table 4 and from our previous paper, the temperature dependence of the interfacial free energy from the combination of CNT prefactor-CNT exponential part was fitted into a widely used equation

$$\sigma_{sl}(T) = \sigma_{sl}(T_1)\ (T/T_1)^n \tag{15}$$

n value of 1.6 in the temperature range from 500 K to 630 K was obtained. The extrapolation to the temperature below 500 K and above 630 K is plotted in Fig. 8. It is an extremely large n value because it expected a number presumably smaller than unity. Nucleation data for the freezing of mercury give n value of *ca*. 0.3 to 0.4. The larger n value for sodium chloride may suggest the unrealistic feature of CNT for the nucleation of sodium chloride under highly super cooled conditions. Besides, as it was pointed out in our previous paper that CNT can not get the solution of interfacial free energy from our 400 K nucleation data

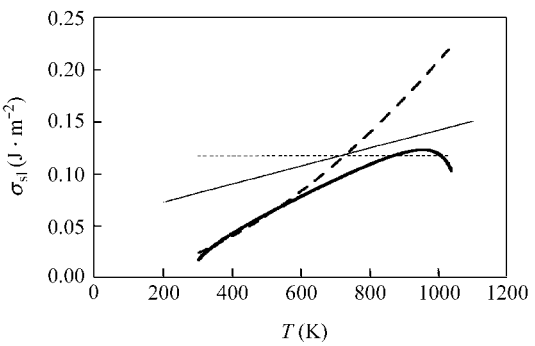

Fig. 8 Interfacial free energy as a function of temperatures derived from different combinations of prefactors and the exponential part. Heavy dash line from CNT-CNT, heavy solid line from DIT-DIT, dash line from GG-CNT, solid line was estimated from Eq. (17) with $k_t = 0.41$.

An almost constant value of σ_{sl} was derived from the GG-CNT combination. This seems against the prediction made by Turnbull[35] and Spaepen[36] that σ_{sl} tends to increase with increasing the temperature.

The diffuse interface thickness δ parameters derived from DIT with nucleation rates are approximately close to a constant value of 0.1520 nm with a fluctuation of 5% in the temperature range from 580 K to 630 K. According to Granasy[30] the δ value can be used to estimate the structure factor k_t. The relationship between the δ and the structure factor k_t is

$$k_t = \delta v_m^{-1/3} \tag{16}$$

where v_m is the volume of a molecule. It leads to a k_t value of 0.41 if the v_m value of 5.2×10^{-28} m^3 is used for liquid molecule. For a series of metalloids the k_t value was found to be *ca*. 0.32, while for metals the value of 0.45 was used. The k_t of 0.41 may be a reasonable value for sodium chloride.

The well known Turnbull empirical equation related with the heat of fusion and interfacial free energy through the structure factor is[37]

$$\sigma_{sl} = k_t \Delta H_{fus} / (V^2 N_A)^{1/3} \tag{17}$$

where N_A is Avogadro's constant, V the molar volume (whether of solid or liquid was not specified). The interfacial free energy was caleulated as a function of temperature by adopting 0.41 for the structure factor, the heat of fusion as a function of temperature estimated from the value at melting poit and the heat capacity difference between liquid and solid from MD simulation, and the liquid volume listed in Table 4. The calculated results are plotted in Fig. 8.

If the free energy barrier to the formation of a critical nucleus from the liquid, ΔG^*, given by CNT [Eq. (6)] and by DIT [Eq. (8)] has the same value at the same temperature, the interfacial free energy from the diffuse interface thickness could be estimated through

$$\sigma_{sl}(\mathrm{DIT}) = (-0.25\delta^3 \Delta G_v^3 \Psi)^{1/3} \tag{18}$$

The calculated results are also plotted in Fig. 8. In the temperature below 650 K range σ_{sl} estimated from DIT behaves the same way as CNT does, while in the temperature above 955 K range σ_{sl} from DIT decreases with increasing the temperature.

No experimental interfacial free energy data were available for sodium chloride therefore it is very difficult to judge which theory gives the most reliable information.

Temperature dependence of nucleation rate

The nucleation rate as a function of temperature derived from three different theories is plotted in Fig. 9 and compared with the result from our MD simulation. All three theories can reproduce the nucleation rate in the temperature range of 500 K to 630 K, however, both CNT and DIT can not be used to interpret the nucleation rate obtained from MD simulation at 400 K. Further studies to the

temperature below 400 K may be helpful to examine the validity results of these theories because the difference in predicted nucleation rate from different theories becomes more clear. On the high temperature end the predicted nucleation rate becomes zero at 1000, 1035 and 1064 K for CNT, DIT and GG theories respectively. Any experimental or simulation results from the high temperature side will be helpful in judging these nucleation theories. We are very eager to explore the possibility of studying this system by the ED experiment.

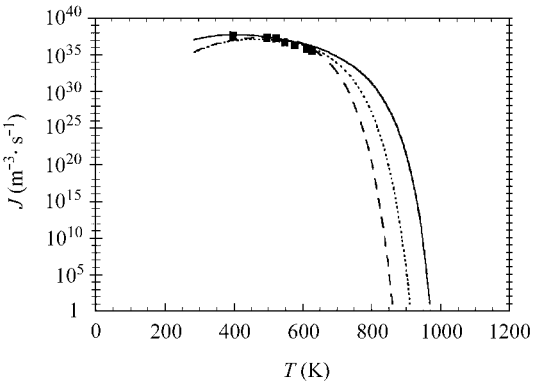

Fig. 9 Nucleation rate as a function of temperature. Squares from MD simulation, solid line from GG-CNT, dash line from CNT-CNT, dot line from DIT-DIT.

To consider the possibility of observing the freezing of sodium chloride from ED experiment based on the MD simulation results, the first consideration will be the time-scale difference between the experiment and the computer simulation. With the present computer power and the time step-size used in molecular dynamics simulation (normally 10 fs per step and 100,000 time steps result in a total time of *ca*. 10^{-9} second, for a cluster with diameter of 2 nm or volume of *ca*. 10^{-27} m^3), it is likely to observe the phase transition of a system withthe nucleation rate around 1036 $m^{-3} \cdot s^{-1}$. The nucleation rates of crystallization of $(NaCl)_{108}$, $(NaCl)_{256}$ and $(NaCl)_{500}$ clusters fall into this range and therefore the nucleation of freezing can be seen in this MD simulation. The limitation of the ED experiment set-up only allows us to investigate phase changes that could be finished within *ca*. 200 μs and the highest time resolution is about 1 μs, cluster diameters are from several nm up to tens nm, and therefore a nucleation rate in the range of 10^{28} to 10^{32} $m^{-3} \cdot s^{-1}$ can be examined by our experiments.

From Fig. 9 it is clear that in order to observe the nucleation in the ED experiment the freezing temperature of the clusters should be controlled between 680 and 750 K from CNT theory, between 700 and 795 K from DIT theory, and between 760 and 846 K from GG theory.

In our previous experiments the freezing temperature of clusters was estimated by the evaporative cooling temperature. Some rules of thumb can be used to approximately estimate the evaporative cooling temperature,[38,39] T_{evp}. For a normal liquid

$$T_{evp} \approx 0.04 \Delta E_{vap}(T_{evp})/R \quad (19)$$

where ΔE_{vap} is the change in internal energy on vaporization at T_{evp}. An alternative approach[1] is to use the temperature at which the vapor pressure of bulk is 0.4 Pa. Based on the empirical formula of vapor pressure[40] $\Delta H_{vap}(T)$ was estimated by Clausius-Claperon equation. Estimates of the evaporative cooling temperature for liquid NaCl clusters from these two approaches are 890 and 880 K respectively. Based on the above information it seems unlikely to observe the nucleation of freezing from the ED experiment. However, the failure of CNT and DIT in interpreting the MD result at 400 K and the constant interfacial free energy estimated from GG theory will remind us that any success of nucleation study of sodium chloride with our ED experiment will be a challenge to current nucleation theories.

Size of critical nuclei

As it is shown in Fig. 5, the number of "fcc unit" sharply increases when the crystal starts to grow. The information about the critical nuclei may be found from the snapshot of the system at the time not very far before the sharply ascending point on such a curve. A rough estimation of the sizes of the critical nuclei from the MD simulation is around 25, 40, and 55 NaCl molecules at temperatures of 580, 615 and 630 K respectively.

From the CNT and GG theory the size of the critical nuclei can be calculated from

$$n^* = 32\pi\sigma_{sl}^3/(3v_m\Delta G_v^2) \quad (20)$$

If the interfacial free enrgy σ_{sl} in Eq. (20) is replaced by Eq. (18), the size of critical nuclei from DIT will be

$$n^* = 8\pi\delta^3\Psi/(3v_m) \quad (21)$$

The calculated sizes of critical nuclei from both CNT and DIT are very small (*ca*. 5 and *ca*. 9 for 580 and 630 K from CNT, *ca*. 4 and *ca*. 7 for 580 and 630 K from DIT), while those from GG theory are slightly bigger (*ca*. 15 and *ca*. 19 for 580 and 630 K respectively).

Concluding remarks

The size and temperature effects on the nucleation rate of crystallization from molten sodium chloride have been studied in the temperature range of 580 to 630 K by MD simulations. The nucleation rate was found to decrease with increasing the cluster size or temperature. Laplace pressure plays the major rule for the size effect on the nucleation rate.

Various nucleation theories were used to interpret the nucleation rates obtained from this report and our previous report on sodium chloride. It was found the interfacial free energy estimated from CNT and DIT increases too fast with

increasing the temperature, while that from GG theory is almost a constant. Although DIT is used with one constant diffuse interface thickness in the temperature range of this study, both DIT and CNT failed to interpret the nucleation rate at 400 K as it was reported in our previous paper.[13] The sizes of the critical nuclei estimated from all the theories are too small.

It seems that all the current nucleation theories could not work very successfully for the freezing of sodium chloride in the temperature range of 400 to 630 K. Further MD simulations on the nucleation of freezing from molten sodium chloride clusters at the temperatures below 400 K and above 630 K are helpful for more thorough evaluation of the current nucleation theories. It will be very exciting to perform ED experiment on this system in order to get the nucleation rate around the evaporative cooling temperatures, and any success in the experiment will be a big challenge to the current nucleation theories.

References

1 Bartell, L. S.; Dibble, T. S. *J. Phys. Chem.* **1991**, *95*, 1159.
2 Dibble, T. S.; Bartell, L. S. *J. Phys. Chem.* **1992**, *96*, 2317.
3 Huang, J.; Bartell, L. S. *J. Phys. Chem.* **1994**, *98*, 4543.
4 Bartell, L. S.; Huang, J. *J. Phys. Chem.* **1994**, *98*, 7455.
5 Huang, J.; Bartell, L. S. *J. Phys. Chem.* **1995**, *99*, 3924.
6 Huang, J.; Lu, W.; Bartell, L. S. *J. Phys. Chem.* **1995**, *99*, 11147.
7 Huang, J.; Lu, W.; Bartell, L. S. *J. Phys. Chem.* **1996**, *100*, 14276.
8 Chen, J.; Bartell, L. S. *J. Phys. Chem.* **1993**, *97*, 10645.
9 (a) Deng, H.; Huang, J. *J. Solid State Chem.* **2001**, *159*, 10.
(b) Ma, M.; Lu, W.; Huang, J. *J. Solid State Chem.* **2002**, *165*, 289.
10 (a) Huang, J.; Bartell, L. S. *J. Mol. Struct.* **2001**, *567*, 145.
(b) Huang, J.; Bartell, L. S. *J. Phys. Chem.* **2002**, *A106*, 2404.
11 Buckle, E. R.; Ubbelohde, A. R. *Proc. Roy. Soc. London* **1960**, *A529*, 325.
12 Huang, J.; Zhu, X.; Bartell, L. S. *J. Phys. Chem.* **1998**, *A102*, 2708.
13 Bartell, L. S.; Huang, J. *J. Phys. Chem.* **1998**, *A102*, 8722.
14 Anastasiou, N.; Fincham, D. *Program MDIONS*, *CCP5 Program Library*, SERC Daresbury Laboratory, Daresbury, UK, **1981**, 8.
15 Westman, S.; Magneli, A. *Acta Chem. Scand.* **1957**, *11*, 1587.
16 Born, B.; Mayer, J. E. *Zeits f. Physik* **1932**, *75*, 1.
17 Huggins, M. L.; Mayer, J. E. *J. Chem. Phys.* **1933**, *1*, 643.
18 Huggins, M. L. *J. Chem. Phys.* **1937**, *5*, 643.
19 Tosi, M. P.; Fumi, F. *J. Phys. Chem. Solids* **1964**, *25*, 45.
20 Tanemura, M.; Hiwatari, Y.; Matsuda, H.; Ogawa, T.; Ogita, N.; Ueda, A. *Prog. Theor. Phys.* **1977**, *58*, 1079.
21 Cape, J. N.; Finney, J. L.; Woodcook, L. V. *J. Chem. Phys.* **1981**, *15*, 2366.
22 Chushak, Y.; Santikary, P.; Bartell, L. S. *J. Phys. Chem. submitted*.
23 Turnbull, D.; Fisher, J. C. *J. Chem. Phys.* **1949**, *17*, 71.
24 Buckle, E. R. *Proc. Roy. Soc. London* **1961**, *A261*, 189 (Part II);
Buckle, E. R. *Proc. Roy. Soc. London* **1961**, *A261*, 197 (Part III).
25 Granasy, L. *Euro. Phys. Lett.* **1993**, *24*, 121.
26 Granasy, L. *J. Non-Cryst. Solids* **1993**, *162*, 301.
27 Granasy, L. *Mater. Sci. Eng.* **1994**, *A178*, 121.
28 Granasy, L. *J. Phys. Chem.* **1995**, *99*, 14183.
29 Grant, M.; Gunton, J. D. *Phys. Rev. B* **1985**, *32*, 7299.
30 Granasy, L. *Symposium on Glass Crystallization*, Florianopollis, Brazil, **1996**, Nov. 4 ~ 6.
31 Harrowell, P.; Oxtoby, D. W. *J. Chem. Phys.* **1984**, *80*, 1639.
32 Shen, Y. C.; Oxtoby, D. W. *J. Chem. Phys.* **1996**, *104*, 4233.
33 Shen, Y. C.; Oxtoby, D. W. *J. Chem. Phys.* **1996**, *105*, 6517.
34 (a) Bartell, L. S. *J. Mol. Struct.* **1998**, *445*, 59.
(b) Bartell, L. S. *Surf. Sci.* **1998**, *397*, 217.
35 Turnbull, D. In *Physics Non-Crystalline Solids*, Ed.: Prins, J. A. E., North Holland, Amsterdam, **1964**, p. 4.
36 Spaepen, F. *Acta Metall.* **1975**, *23*, 729.
37 Turnbull, D. *J. Appl. Phys.* **1950**, *21*, 1022.
38 Reiss, H.; Mirabel, P.; Whetten, R. L. *J. Phys. Chem.* **1988**, *92*, 7241.
39 Antonow, G. *J. Chim. Phys.* **1907**, *5*, 372.
40 Gspann, J. In *Physics of Electronic and Atomic Collisions*, Eds.: Datz, S., North-Holland, New York, **1982**.
41 Eucken, A. *Ann. Physik* **1911**, *34*, 185.
42 Mccarthy, K. A.; Ballard, S. S. *J. Appl. Phys.* **1960**, *31*, 1410.
43 (a) Bonacha, A. Z.; Bockris, J. O'M.; Kitchener, A. *Proc. Roy. Soc. London* **1957**, *A241*, 554.
(b) Bockris, J. O'M.; Hooper, G. W. *Discuss Faraday Soc.* **1961**, *32*, 218.
44 International Critical Tables of Numerical Data, 1947—1971.

(E0305297 SONG, J. P.; FAN, Y. Y.)